Arch. Mech., **61**, 3–4, pp. 283–307, Warszawa 2009

Notched concrete beams under bending – calculations of size effects within stochastic elasto-plasticity with non-local softening

J. BOBIŃSKI, J. TEJCHMAN, J. GÓRSKI

Faculty of Civil and Environmental Engineering
Gdańsk University of Technology
Narutowicza 11/12
80-233 Gdańsk-Wrzeszcz, Poland
e-mails: bobin@pg.gda.pl, tejchmk@pg.gda.pl, jgorski@pg.gda.pl

Numerical FE investigations of a deterministic and statistical size effect in notched concrete beams of a similar geometry under three-point bending were performed. The FE analyses were carried out with four different beam sizes. Deterministic calculations were performed assuming constant values of tensile strength. In turn, in statistical calculations, the tensile strength took the form of random spatial fields described by a truncated Gaussian random distribution. In order to reduce the number of stochastic realizations without loosing the accuracy of the calculations, Latin hypercube sampling was applied. The numerical results were compared with the corresponding laboratory tests. The numerical outcomes show that the bearing capacity of beams and their ductility increase with decreasing specimen size. If the distribution of the tensile strength is stochastically distributed, the mean beam strength is always smaller than the deterministic value.

Key words: concrete, Latin hypercube sampling, notched beams, non-local softening, size effect, strain localization.

1. Introduction

The size effect phenomenon (nominal strength varies with the size of structure) is an inherent property of the behaviour of many engineering materials. In the case of cementitious materials, both the nominal strength and material brittleness (ratio between the energy consumed during the fracture process after and before the peak) decrease with increasing element size under tension (Walraven and Lehwalter [43], Wittmann *et al.* [46], Bažant and Chen [3], Bažant and Planas [4], van Vliet [48], Chen *et al.* [16], Le Bellego *et al.* [30], van Mier and van Vliet [34], Vořechovský [49]). Thus, concrete becomes perfectly brittle on a sufficiently large scale. The results of laboratory tests which are scaled versions of the actual structures cannot be directly transferred to them. The physical understanding of size effects is of major importance for civil

engineers, who try to extrapolate experimental outcomes at laboratory scale to results which can be used in big scale situations. Since large structures are beyond the range of testing in laboratories, their design has to rely on a realistic extrapolation of testing results with smaller sizes.

Two size effects are of a major importance: deterministic and the statistical one. The first one is caused by the fact that fracture is preceded by the formation of a region with strain localization of a certain width (in the form of a fracture process zone FPZ), which cannot be appropriately scaled in laboratory tests. Strain localization is not negligible for the cross-section dimensions and is large enough to cause significant stress redistribution in the structure. The specimen strength increases with increasing ratio l_c/L (l_c – characteristic length of the micro-structure influencing both the thickness and spacing of localized zones, L – specimen size). In turn, a statistical (or stochastic) effect is caused by the spatial variability/randomness of local material strength. In spite of many experiments exhibiting the noticed size effect in concrete and reinforced concrete elements under different loading types (Walraven and Lehwalter [43], Bažant and Planas [4], Bažant [6], Bažant and Yavari [7], Yu [51]), the size effect is not always taken into account in practical design of engineering structures (what may contribute to their failure, Bažant and Planas [4], Yu [51]).

For brittle materials, there are only a few reliable approaches to describe the size effects. For example, two size effect laws proposed by Bažant (Bažant and Planas [4], Bažant [6]) for geometrically similar structures allow one to take into account the size difference by determining the tensile strength of structures without notches and preexisting large cracks (the so-called type 1 size effect), and of notched structures (the so-called type 2 size effect). In the first type structures, the maximum load is reached as soon as a macroscopic crack initiates from the fully formed FPZ. In the second type structures, cracks grow in a stable manner prior to the maximum load. Only the first type of structures is significantly affected by material randomness causing a pronounced statistical size effect. The material strength is bound for small sizes by a plasticity limit, whereas for large sizes the material follows the linear elastic fracture mechanics. The most known statistical theory is the Weibull's [45] theory (called also the weakest link theory) which is based on the distribution of flaws in a material. It postulates that a structure is as strong as its weakest component. The structure fails when its strength is exceeded, since a stress redistribution is not considered. This model is not able to account for a spatial correlation between local material properties. Another approach to the size effect was proposed by Carpinteri *et al.* [15], which was based on the multi-fractality of a fracture surface which increased with spreading disorder of the material in large structures. In this approach, the material strength is bound for small and large sizes by the plasticity limit. The nominal strength decreases in a hyperbolic form with increasing

structure size. According to BAŽANT and YAVARI [7], the cause of size effect is energetic-statistical not fractal. The fits of the size effect law by BAŽANT [6] and the multi-fractal scaling law by CARPINTIERI *et al.* [15] to experimental data for concrete elements (VAN VLIET [48]) have shown that both laws are similar only for experiments at the laboratory scale, but significantly differ when the structure is very small or very large.

The goal of the numerical simulations in this paper is to investigate a deterministic and statistical size effect on flexural resistance in notched concrete beams of a similar geometry under quasi-static three-point bending, by considering the influence of strain localization. A finite element method with an elasto-plastic constitutive model using Rankine'a criterion with non-local softening (MARZEC *et al.* [32], MAJEWSKI *et al.* [31]) was used which is able to properly capture strain localization. Two-dimensional calculations were performed with four different concrete beam sizes of a similar geometry. Deterministic calculations were performed assuming constant values of tensile strength. In turn, statistical analyses were carried out with spatially correlated homogeneous distributions of tensile strength which were assumed to be random. Truncated Gaussian random tensile strength fields were generated using a conditional rejection method (WALUKIEWICZ *et al.* [44]) for correlated random fields. The approximate results were obtained using a Latin hypercube sampling method (MCKAY *et al.* [33], BAŽANT and LIN [2], FLORIAN [18], HUNTINGTON and LYRINTZIS [25]) belonging to a group of variance reduced Monte Carlo methods (HURTADO and BARBAT [26]). This approach enables a significant reduction of the sample number without loosing the accuracy of calculations. The numerical results of load-displacements diagrams were compared with the corresponding laboratory tests performed by LE BELLEGO *et al.* [30]. The effect of the correlation length was also investigated (only in a small-size beam).

The deterministic calculations for the similar boundary value problems were performed among others by PAMIN and DE BORST [35] and PAMIN [36] with a second-gradient elasto-plastic model, SIMONE *et al.* [39] with a second-gradient damage model, and BOBIŃSKI and TEJCHMAN [11, 12], using elasto-plastic model and damage model with non-local softening. In turn, the combined statistical and deterministic size effects were simulated by CARMELIET and HENS [14], FRANTZISKONIS [19], GUTIÉRREZ and DE BORST [21], GUTIÉRREZ [22], VOŘECHOVSKÝ [49], BAŽANT *et al.* [8] and YANG and XU [50]. The most comprehensive combined calculations were performed by VOŘECHOVSKÝ [49] for unnotched concrete specimens under uniaxial tension with a micro-plane material model and crack band model, using Latin hypercube sampling. A squared exponential autocorrelation function with the correlation length of 80 mm was used. His results show that the strength of many specimens, with parameters which were obtained from random sampling, could be larger than a deterministic one in

small specimens, in contrast to large specimens which rather obeyed the weakest link model. The difference between a deterministic material strength and a mean statistical strength grew with increasing size. The structural strength exhibited a gradual transition from Gaussian distribution to Weibull distribution at increasing size. As the ratio of autocorrelation length and specimen size decreased, the ratio of spatial fluctuation of random field realizations grew. In the work by Yang and Xu [50], a heterogeneous cohesive crack model to predict macroscopic strength of materials based on meso-scale random fields of fracture properties was proposed. One four-point concrete notched beam subjected to mixed-mode fracture was modeled. Effects of various important parameters on the crack paths, peak loads, macroscopic ductility and overall reliability, including the variance of random fields, the correlation length, and the shear fracture resistance, were investigated and discussed.

Our paper follows the research presented by Vořechovský [49] by using an alternative stochastic finite element method. In contrast to his simulations, we have dealt here in the first step with notched elements of similar geometry. The innovations in the present paper are the following: a) a more sophisticated regularization technique was used in the softening regime, namely non-local theory, which ensures entirely mesh-independent results with respect to load-displacement diagrams and widths of localized zones (in contrast to the crack band model which provides only mesh-independent load-displacement diagrams), b) our FE calculations were carried out with a different boundary value problem (notched beams under bending), and c) an original method of the random field generation with a different homogeneous correlation function was used.

The outline of the present paper is as follows. First, after the introduction (Sec. 1), the employed constitutive elasto-plastic model with non-local softening is summarized (Sec. 2). The simulation of discrete random fields is described in Sec. 3. Information about the finite element discretization and boundary conditions are given in Sec. 4. The numerical results of the deterministic and statistical size effects are discussed in Sec. 5. Conclusions and future plans are described in Sec. 6.

2. Constitutive elasto-plastic model with non-local softening

To describe the behaviour of concrete under tension during three-point bending, a Rankine criterion was used with the yield function f, with isotropic softening defined as:

$$f = \max\{\sigma_1, \sigma_2, \sigma_3\} - \sigma_t(\kappa), \tag{2.1}$$

where: σ_i – principal stress, σ_t – tensile yield stress and κ – softening parameter equal to the maximum principal plastic strain ε_1^p. The associated flow rule was

assumed. To model concrete softening under tension, the exponential curve by HORDIJK [24] was chosen:

$$\sigma_t(\kappa) = f_t[(1 + (A_1\kappa)^3)\exp(-A_2\kappa) - A_3\kappa], \tag{2.2}$$

where f_t stands for the tensile strength of the concrete $f_t = 3.6$ MPa). The parameters A_1, A_2 and A_3 were:

$$A_1 = \frac{c_1}{\kappa_u}, \qquad A_2 = \frac{c_2}{\kappa_u}, \qquad A_3 = \frac{1}{\kappa_u}(1 + c_1^3)\exp(-c_2), \tag{2.3}$$

wherein $\kappa_u = 0.005$ denotes the ultimate value of the softening parameter, and the constants c_i are: $c_1 = 3$ and $c_2 = 6.93$. The modulus of elasticity was assumed to be $E = 38.5$ GPa and the Poisson ratio was $\nu = 0.24$. The edge and vertex in Rankine yield function were taken into account by the interpolation of 2–3 plastic multipliers according to the Koiter's rule.

To properly describe strain localization, to preserve the well-posedness of the boundary value problem, to obtain mesh-independent results and to include a characteristic length of micro-structure for simulations of a deterministic size effect, a non-local theory was used as a regularisation technique (PIJAUDIER-CABOT and BAŽANT [37], BAŽANT and JIRASEK [5]). A principle of a local action does not take place any more. Thus, any variable at a certain material point depends not only on the state variables at that point but also on the distribution of state variables in a finite neighbourhood of the considered point. Usually it is sufficient to treat non-locally only one variable controlling material softening or degradation (BAŽANT and JIRASEK [5]). In the calculations, the softening parameter κ was assumed to be non-local ($\bar{\kappa}$)

$$\bar{\kappa}(\mathbf{x}) = \frac{\int_V \omega(\|\mathbf{x} - \boldsymbol{\xi}\|)\kappa(\boldsymbol{\xi})d\boldsymbol{\xi}}{\int_V \omega(\|\mathbf{x} - \boldsymbol{\xi}\|)d\boldsymbol{\xi}}, \tag{2.4}$$

where $\bar{\kappa}(\mathbf{x})$ is the non-local softening parameter, V – the volume of the body, $\mathbf{x}$ – the coordinates of the considered (actual) point, $\boldsymbol{\xi}$ – the coordinates of the surrounding points in a certain neighborhood of the considered point and ω – the weighting function. The softening non-local parameters $\bar{\kappa}$ near the boundaries were calculated also on the basis of Eq. (2.4) (which satisfies the normalizing condition). As a weighting function ω, a Gauss distribution function was used

$$\omega(r) = \frac{1}{l_c\sqrt{\pi}}e^{-(r/l_c)^2}, \tag{2.5}$$

where r is a distance between two material points. The averaging in Eq. (2.5) is restricted to a small representative area around each material point (the influence of points at the distance of $r = 3l_c$ is only of 0.01%), Fig. 1. A characteristic length is usually related to the micro-structure of the material (e.g. maximum

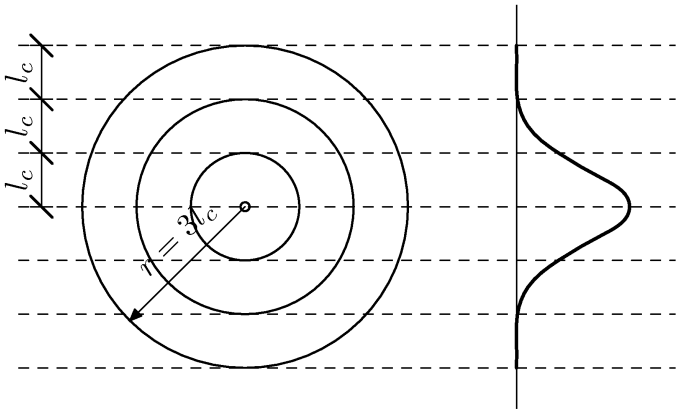

FIG. 1. Region of the influence of a characteristic length l_c and weighting function ω.

aggregate size). It is determined with an inverse identification process of experimental data (LE BELLEGO *et al.* [30]). However, the determination of the representative characteristic length of micro-structure l_c is very complex in concrete, since strain localization can include a mixed mode (cracks, shear zones) and the characteristic length (which is a scalar value) is related to the fracture process zone with a certain volume. In turn, other researchers conclude that the characteristic length depends upon the boundary value problem (FERRARA and DI PRISCO [17]). The width of the fracture process zone increases according to e.g. PIJAUDIER-CABOT *et al.* [38], but decreases after e.g. SIMONE *et al.* [39]). It depends also on the choice of the weighting function.

The FE-analyses show that a classical non-local assumption (Eq. (2.4)) does not fully regularize a boundary value problem in elasto-plasticity (BRINKGREVE [13], BAŽANT and JIRASEK [5], BOBIŃSKI and TEJCHMAN [10]). Therefore, a modified formula (according to BRINKGREVE [13]) was used to calculate the nonlocal softening parameter

$$\bar{\kappa}(\mathbf{x}) = (1-m)\kappa(\mathbf{x}) + m\frac{\int_V \omega(\|\mathbf{x}-\boldsymbol{\xi}\|)\kappa(\boldsymbol{\xi})d\boldsymbol{\xi}}{\int_V \omega(\|\mathbf{x}-\boldsymbol{\xi}\|)d\boldsymbol{\xi}}, \tag{2.6}$$

where m denotes an additional parameter controlling the size of the localized plastic zone and the distribution of the plastic strain. For $m = 0$, a local approach is obtained and for $m = 1$, a classical non-local model is recovered. If the parameter $m > 1$, the influence of non-locality increases and the localized plastic region reaches a finite mesh-independent size (BOBIŃSKI and TEJCHMAN [10]). To simplify the calculations, the non-local rates were replaced by their approximation $\Delta\kappa_i^{est}$ calculated on the basis of the known total strain increment values:

$$\Delta\bar{\kappa}(\mathbf{x}) \approx \Delta\kappa(\mathbf{x}) + m\left(\frac{\int_V \omega(\|\mathbf{x}-\boldsymbol{\xi}\|)\Delta\kappa^{est}d\boldsymbol{\xi}}{\int_V \omega(\|\mathbf{x}-\boldsymbol{\xi}\|)d\boldsymbol{\xi}} - \Delta\kappa^{est}(\mathbf{x})\right) \tag{2.7}$$

with $\Delta\kappa^{est}(\mathbf{x}) = \Delta\varepsilon_1(\mathbf{x})$ ($\Delta\varepsilon_1$ the increment of principal total strain). Equation (2.7) enables to 'freeze' the non-local influence of the neighbouring points and to determine the actual values of the softening parameters, using the same procedures as in a local formulation. The calculations were carried out with $l_c = 5$ mm and $m = 2$ on the basis of other FE calculations (BOBIŃSKI and TEJCHMAN [10], MARZEC *et al.* [32], MAJEWSKI *et al.* [31]) and experiments using a DIC technique (KOZICKI and TEJCHMAN [29], SKARZYŃSKI *et al.* [40]).

The 2D and 3D non-local model was implemented in the commercial finite element code Abaqus [1] with the aid of subroutine UMAT (user constitutive law definition) and UEL (user element definition) for efficient computations (BOBIŃSKI and TEJCHMAN [10]). For the solution of the non-linear equation of motion governing the response of a system of finite elements, the initial stiffness method was used with a symmetric elastic global stiffness matrix. The calculations were carried out using a large-displacement analysis available in the Abaqus finite element code [1] (although the influence of such analysis was negligible). In this method, the current configuration of the body was taken into account. The Cauchy stress was taken as the stress measure. The conjugate strain rate was the rate of deformation. The rotation of the stress and strain tensor was calculated by the Hughes–Winget method [24]. The non-local averaging was performed in the current configuration.

To capture a snap-back behaviour in a very large size beam, the so-called arc-length technique was used. The actual load vector $\mathbf{P}$ was defined as $\lambda\mathbf{P}_{\max}$ where λ – multiplier and $\mathbf{P}_{\max}$ – maximum constant load vector. In general, the determination of the length of the arc the $\mathbf{P}-\mathbf{u}$ space ($\mathbf{u}$ – displacement vector) involves the displacements of all nodes (as e.g. the Riks method available in Abaqus Standard [1]). However, for problems involving strain localization, it is more suitable to use an indirect displacement control method, where only selected nodal displacements are considered to formulate an additional condition in the $\mathbf{P}-\mathbf{u}$ space. The horizontal distance between two nodes lying on opposite sides of the notch was chosen as a control variable *CMOD* (crack mouth open displacement). The indirect displacement algorithm was implemented with the aid of two identical and independent FE-meshes and some additional node elements, to exchange the information about the displacements between these meshes.

3. FE-input data

3.1. Deterministic calculations

The two-dimensional FE-calculations of simply supported notched beams with free ends (assuming constant values of tensile strength f_t) were performed

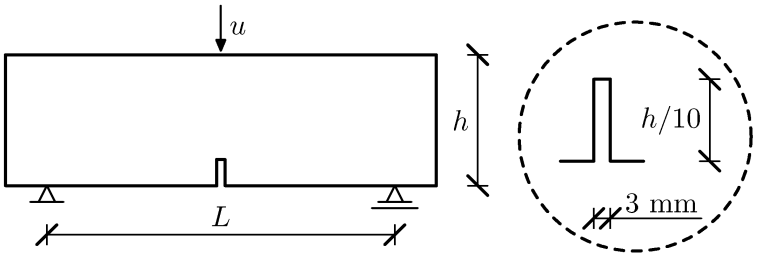

Fig. 2. Notched beams used for calculations (with $L = 3 \times h$).

with 4 different beam sizes of a similar geometry $h \times L_t$: 8×32 cm^2 (called small size beam), 16×64 cm^2 (called medium size beam), 32×128 cm^2 (called large size beam) and 192×768 cm^2 (called very large size beam) (h – beam height, L_t – total beam length), Fig. 2. The span length L was equal to $3h$ for all beams. The size of the first 3 beams was similar as in the corresponding experiments carried out by Le Bellego *et al.* [30]. The quadrilateral elements divided into triangular elements were used to avoid volumetric locking. 7628 triangular (small size beam), 14476 (medium size beam), 28092 (large size beam) and 104310 triangular elements were used, respectively. The mesh was particularly very fine in the region of a notch (Fig. 3) to properly capture strain localization in concrete (where the element size was equal to $1/3 \times l_c$). The ratio between the width of this region and the beam length was always the same. A quasi-static deformation of a small, medium and large beam was imposed through a constant vertical displacement increment Δu prescribed at the upper mid-point of the beam top. In the case of a very large beam (to capture the snap-back behavior), a procedure described in Sec. 2 was used.

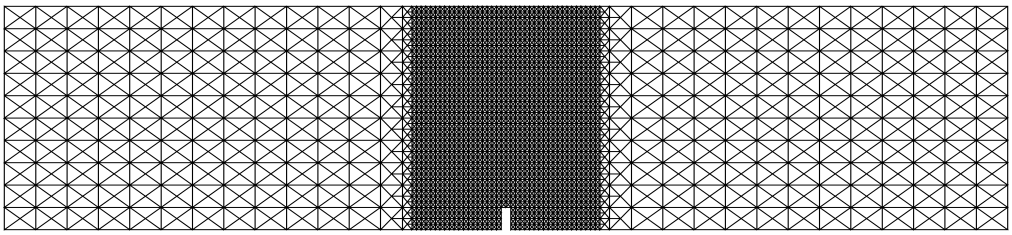

Fig. 3. FE mesh in the case of a medium size beam.

3.2. Statistical calculations

3.2.1. Latin sampling method. In the paper the Monte Carlo method was used. Application of the method in stochastic problems of mechanics requires the following steps: simulation of random variables or fields describing the problem

under consideration (variability of material parameters, initial imperfections in structure geometrics and others), solution of the problem for each simulated realization, creation of a set of results and its statistical description. Contrary to stochastic finite element codes, the Monte Carlo method does not impose any restriction to the solved random problems. Its only limitation is the time of calculations. For example, to reproduce exactly the input random data of initial geometric imperfection of a shell structure problem, at least 2000 random samples should be used (BIELEWICZ and GÓRSKI [9]). Any nonlinear calculations for such a number of initial data are, however, impossible due to excessive computation times. To determine a minimal, but sufficient number of samples (which allows one to estimate the results with a specified accuracy), a convergence analysis of the outcomes was proposed (GÓRSKI [20]). It was estimated that in case of various engineering problems, only ca. 50 realizations had to be considered. For example, in the shell structure limit load analysis (GÓRSKI [20]), the change of the error of limit load mean values between 50 and 150 samples equaled 2% and the standard deviations error was 12%. A further decrease of sample numbers can be obtained using Monte Carlo variance reduction methods.

In the papers by TEJCHMAN and GÓRSKI [41, 42], two methods: a stratified and a Latin sampling method were considered. It should be pointed up that these methods were not used for the generation of two-dimensional random fields as, for example, in the paper by VOŘECHOVSKÝ [49], but for their classification. For that reason, the single realization was generated according to the initial data, i.e. the theoretical mean value and the covariance matrix was exactly reproduced. The statistical calculations according to the proposed version of the Latin sampling method were performed in two steps (TEJCHMAN and GÓRSKI [41, 42]). First, an initial set of random samples was generated in the same way as in the case of a direct Monte Carlo method. Next, the generated samples were classified and arranged in increasing order according to the chosen parameters (i.e. their mean values and the gap between the lowest and the highest values of the fields). From each subset defined in this way, only one sample was chosen for the analysis. The selection was performed in agreement with the theoretical background of the Latin sampling method. The numerical calculations were performed only for these samples. It was proved that using the Latin sampling variance reduction method, the results can be properly estimated by several realizations only (e.g. 12–15) (TEJCHMAN and GÓRSKI [41, 42]).

To generate the random field, the conditional-rejection method described by WALUKIEWICZ *et al.* [44], BIELEWICZ and GÓRSKI [9], GÓRSKI [20]. TEJCHMAN and GÓRSKI [41], and TEJCHMAN and GÓRSKI [42] was used. The method makes it possible to simulate any homogeneous or non-homogeneous truncated Gaussian random field described on regular or irregular spatial meshes. The

simulation process was based on the original, conditional rejection method of generation. An important role in the calculations was played by the propagation base scheme covering sequentially the mesh points and the random field envelope, which allowed one to fulfill the geometric and boundary conditions of the structure of the model. Random fields of practically unlimited sizes could be generated.

3.2.2. Random field data in the problem of beam bending. Various properties of concrete may be considered as randomly distributed. In the present work, only fluctuations of its tensile strength were taken into account. Two parameters describing the random field should be chosen, i.e. the distribution of the random variable in a single point of the field and a function defining the correlation between these points.

In the work, the distribution of a single random variable took the form of a truncated Gaussian function with the mean concrete tensile strength of $\bar{f}_t = 3.6$ MPa. Additionally, it was assumed that the concrete tensile strength values changed between $f_t = 1.6$ MPa and $f_t = 5.6$ MPa ($f_t = 3.6 \pm 2.0$ MPa). To fulfil this condition, the standard deviation $s_{f_t} = 0.424$ MPa was used in the calculations. The coefficient of variations describing the field scattering was $\text{cov} = s_{f_t}/\bar{f}_t = 0.118$ ($\bar{f}_t$ – the mean tensile strength). It is easy to notice that $5s_{f_t} = 5 \times 0.424 = 2.12$ MPa and the cut of variables did not change the theoretical Gauss distribution distinctly (Fig. 4). The Irvin's characteristic length EG_f/f_t^2, (G_f – tensile fracture energy) which controls the length of the fracture process zone, BAŽANT and PLANAS [4]), varied between 0.100 m and 0.351 m.

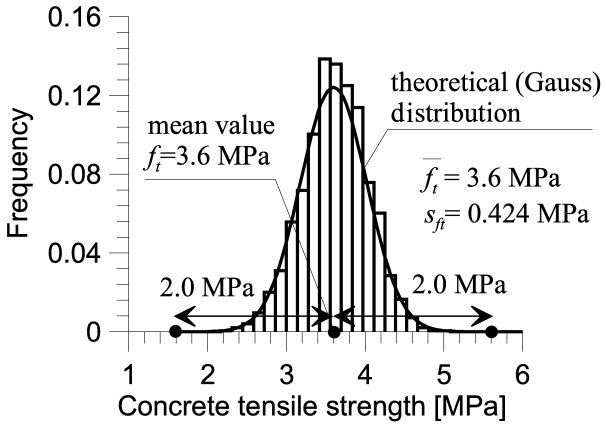

FIG. 4. Distribution of the concrete strength values for a single point of the mesh.

Randomness of tensile strength f_t has to be described by a correlation function. Due to lack of the appropriate data, the correlation function is usually

chosen arbitrarily. It is evident that the fluctuation of any material parameters should be described by a homogeneous function, which confirms that the correlation between random material variables vanishes when the random point distance increases. Any non-homogeneous correlation function, for example Wiener or Brown, defines strong correlation between every point of the field, and such a definition of material parameters is unrealistic. The simplest choice is a standard first-order correlation function $K(x_1, x_2) = e^{-\lambda_{x_1}\Delta x_1} e^{-\lambda_{x_2}\Delta x_2}$. Here, the following, more general, second-order, homogeneous correlation function was adopted (BIELEWICZ and GÓRSKI [9])

$$K(\Delta x_1, \Delta x_2) = s_{f_t}^2 \times e^{-\lambda_{x_1}\Delta x_1}(1 + \lambda_{x_1}\Delta x_1) e^{-\lambda_{x_2}\Delta x_2}(1 + \lambda_{x_2}\Delta x_2), \tag{3.1}$$

where Δx_1 and Δx_2 are the distances between two field points along the horizontal axis x_1 and vertical axis x_2, λ_{x_1} and λ_{x_2} are the decay coefficients (damping parameters) characterizing a spatial variability of the specimen properties (i.e. describe the correlation between the random field points). The second-order homogeneous function (Eq. (3.1)) proved to be very useful in engineering calculations (KNABE *et al.* [27]).

In finite element methods, continuous correlation function (Eq. (3.1)) has to be represented by the appropriate covariance matrix. For this purpose, the procedure of local averages of the random fields proposed by VANMARCKE [47] was adopted. After an appropriate integration of the function (Eq. (3.1)), the following expression describing the variances D_w and covariances K_w were obtained (KNABE *et al.* [27]):

$$\begin{aligned} D_w(\Delta x_1, \Delta x_2) = {} & \frac{2}{\lambda_{x_1}\Delta x_1} s_{f_t}^2 \left[2 + e^{-\lambda_{x_1}\Delta x_1} - \frac{3}{\lambda_{x_1}\Delta x_1}(1 - e^{-\lambda_{x_1}\Delta x_1}) \right] \\ & \times \frac{2}{\lambda_{x_2}\Delta x_2} s_{f_t}^2 \left[2 + e^{-\lambda_{x_2}\Delta x_2} - \frac{3}{\lambda_{x_2}\Delta x_2}(1 - e^{-\lambda_{x_2}\Delta x_2}) \right], \end{aligned} \tag{3.2}$$

$$\begin{aligned} & K_w(\Delta x_1, \Delta x_2) \\ & = \frac{e^{\lambda_{x_1}\Delta x_1}}{(\lambda_{x_1}\Delta x_1)^2} s_{f_t}^2 \{ [\cos(\lambda_{x_1}\Delta x_1) - \sin(\lambda_{x_1}\Delta x_1)] + 2\lambda_{x_1}\Delta x_1 - 1 \} \\ & \times \frac{e^{\lambda_{x_2}\Delta x_2}}{(\lambda_{x_2}\Delta x_2)^2} s_{f_t}^2 \{ [\cos(\lambda_{x_2}\Delta x_2) - \sin(\lambda_{x_2}\Delta x_2)] + 2\lambda_{x_2}\Delta x_2 - 1 \}. \end{aligned} \tag{3.3}$$

We took mainly into account a strong correlation of the tensile strength f_t in horizontal direction $\lambda_{x_1} = 1.0$ 1/m and a weaker correlation in the vertical directions $\lambda_{x_2} = 3.0$ 1/m in Eq. (3.1) (due to the way of specimen's preparation). In this way, the layers formed during the concrete placing were modeled. The range of significant correlation was approximately 80 mm in the horizontal direction and 30 mm in the vertical direction (the correlation distances for the normalized

correlation function are presented in Fig. 5). The smaller is the lambda parameter, the shorter will be the correlation range. The dimension of the random field was identical as the finite element mesh. The same random values were assumed in 4 neighboring triangular elements.

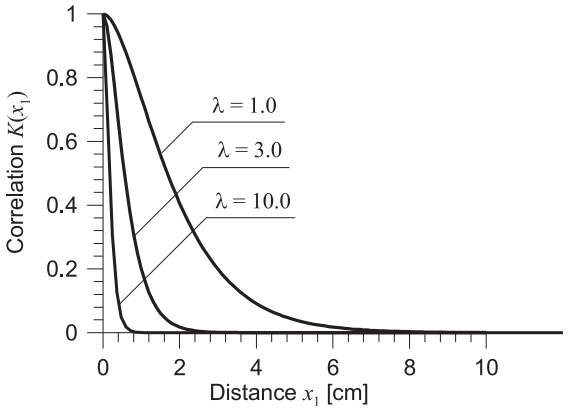

Fig. 5. The correlation distances for different coefficients λ [1/m].

Using the conditional-rejection method, 2000 field realizations of the initial void ratio tensile strength were generated. Next, the generated fields were classified according to two parameters: the mean value of the tensile strength and the gap between the lowest and the highest value of the tensile strength. The joint probability distribution (so-called "ant hill") is presented in Fig. 6. One dot represents one random vector described by its mean value and the difference between its extreme values. The two variable domains were divided into 12 intervals of equal probabilities (see vertical and horizontal lines in Fig. 6). Next,

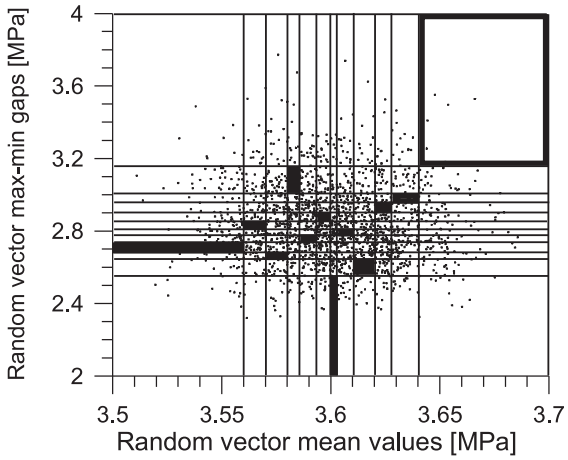

Fig. 6. Selection of 12 pairs of random samples using Latin hypercube sampling: 1–4, 2–7, 3–3, 4–11, 5–5, 6–8, 7–1, 8–6, 9–2, 10–9, 11–10 and 12–12.

according to the Latin hypercube sampling assumptions, 12 random numbers in the range 1-12 were generated (one number appeared only once) using the uniform distribution. The generated numbers formed the following 12 pairs: 1–4, 2–7, 3–3, 4–11, 5–5, 6–8, 7–1, 8–6, 9–2, 10–9, 11–10 and 12–12. According to these pairs, the appropriate areas (subfields) were selected (they are presented as rectangles in Fig. 6). From each subfield, only one realization was chosen and used as the input data to the FEM calculations. In this way the results of 12 realizations were analyzed. Figure 7 shows a stochastic distribution of tensile strength in one concrete beam in the area close to the notch.

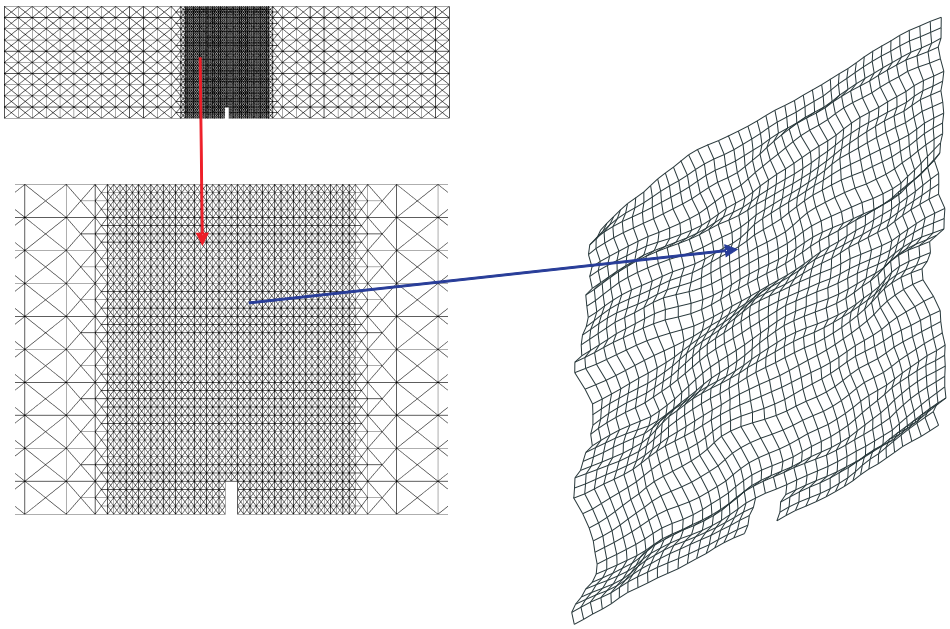

FIG. 7. Stochastic distribution of tensile strength f_t close to the notch in small size beam (strong correlation, small standard deviation).

4. FE-results

4.1. Deterministic size effect

Figure 8 shows the evolution of the calculated vertical force P versus the vertical beam deflection u and normalized vertical force $PL/tf_t(0.9h)^2$ versus the normalized vertical beam displacement u/h, for four different beam heights h: 8 cm, 16 cm, 32 cm and 192 cm, with constant values of tensile strength of $f_t = 3.6$ MPa. The depth of the specimen was equal to $t = 4$ cm (as in laboratory experiments). The calculations were performed under plane strain conditions (the differences between the results obtained within Rankine plasticity under plane stress and plane strain conditions are insignificant). A distribution of the

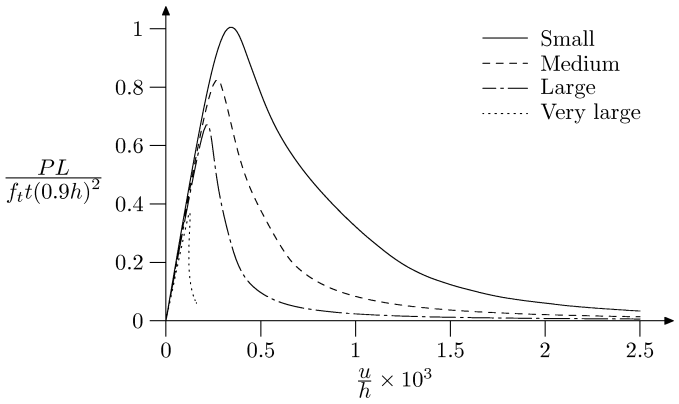

Fig. 8. Normalized force-displacement curves with constant values of tensile strength for 4 notched beams under three-point bending.

non-local softening parameter is shown close to the notch (Fig. 9). Moreover, the numerical results of a deterministic size effect compared to the size effect model by Bažant for notched concrete specimens (Bažant and Planas [4]) are shown (Fig. 10).

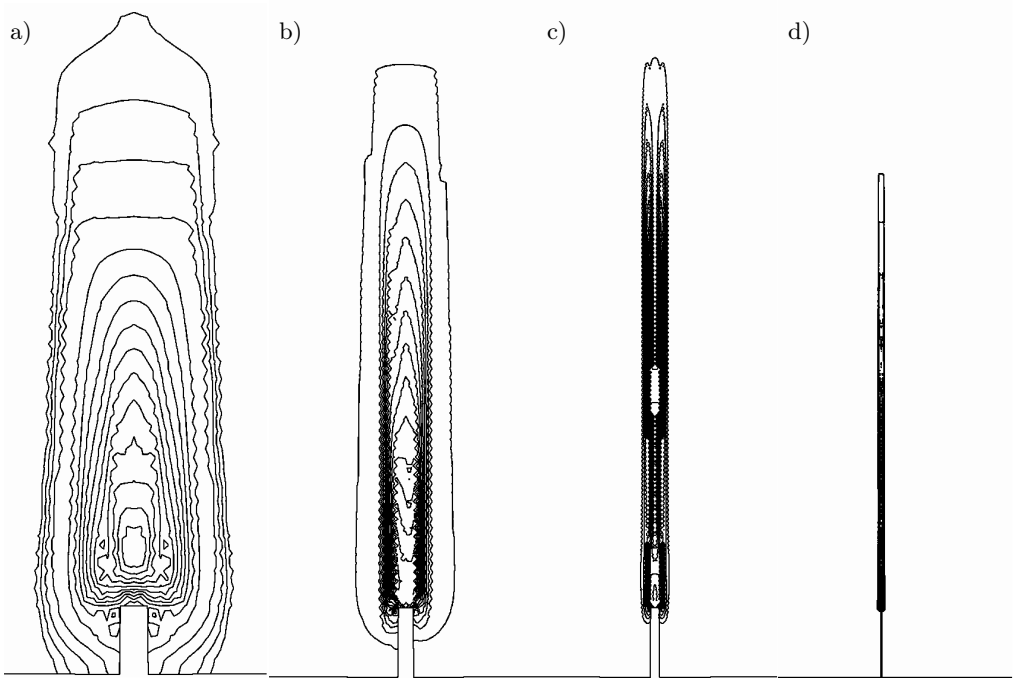

Fig. 9. Calculated contours of non-local softening parameter $\bar{\kappa}$ above the notch for three-point bending of small (a), medium (b), large (c), and very large (d) concrete beam (constant values of tensile strength).

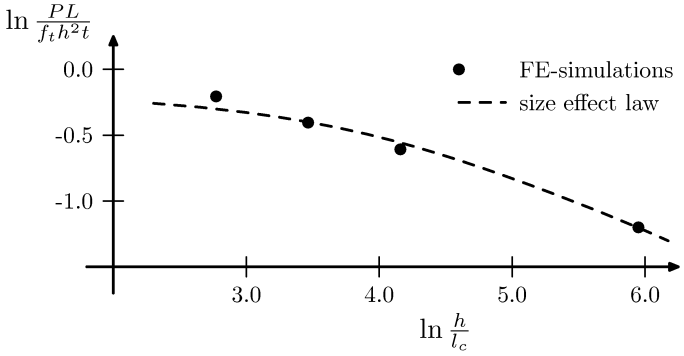

FIG. 10. Relationship between the calculated normalized concrete strength $\ln\sigma = \ln[PL/(f_t h^2 t)]$ and ratio $\ln(h/l_c)$, compared to the size effect law by Bažant (BAŽANT and PLANAS [4]) for constant values of tensile strength.

The beam strength and beam brittleness obviously increases with increasing beam size. This pronounced deterministic size effect is in agreement with the size effect model by Bažant (BAŽANT and PLANAS [4]). For a very large size beam, a so-called snap-back behaviour occurred (decrease of strength with decreasing deformation). The mean width of a localized zone above the notch was 15.08 mm (h = 8 cm), 15.10 mm (h = 16 cm), 18.02 mm (h = 32 cm) and 18.05 mm (h = 192 cm) at $u/h = 1.000‰$, $0.494‰$, $0.234‰$ and $0.105‰$, respectively.

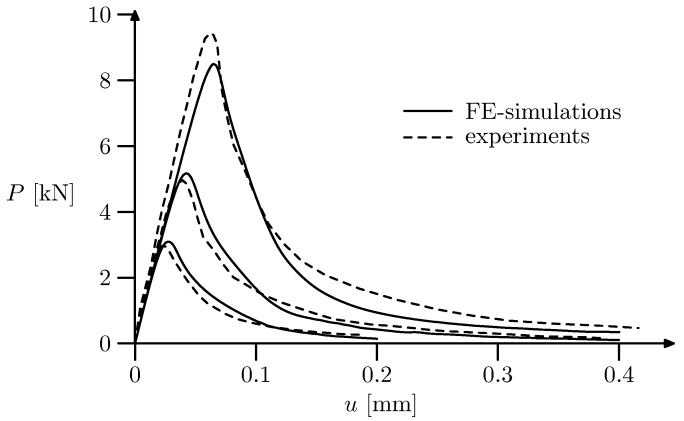

FIG. 11. The load-displacement curves from FE-calculations with constant values of tensile strength compared to the experiments by LE BELLEGO *et al.* [30]: h = 8 cm, h = 16 cm and h = 32 cm.

The calculated vertical forces for a small, medium and large beam are in good accordance with the experiments by LE BELLEGO *et al.* [30] (Fig. 11). The calculated width of the localized zone was similar as in experiments, i.e. about 20 mm (on the basis of acoustic emission, PIJAUDIER-CABOT *et al.* [38]).

4.2. Statistical size effect

12 selected random samples using Latin hypercube sampling are shown in Fig. 6 ($\lambda_{x_1} = 1.0$ 1/m, $\lambda_{x_2} = 3.0$ 1/m, $s_{f_t} = 0.424$ MPa). The 12 different evolutions of the vertical force P versus the vertical displacement u are shown in Fig. 12 for 3 different beam heights h: 8 cm (small beam), 32 cm (large beam)

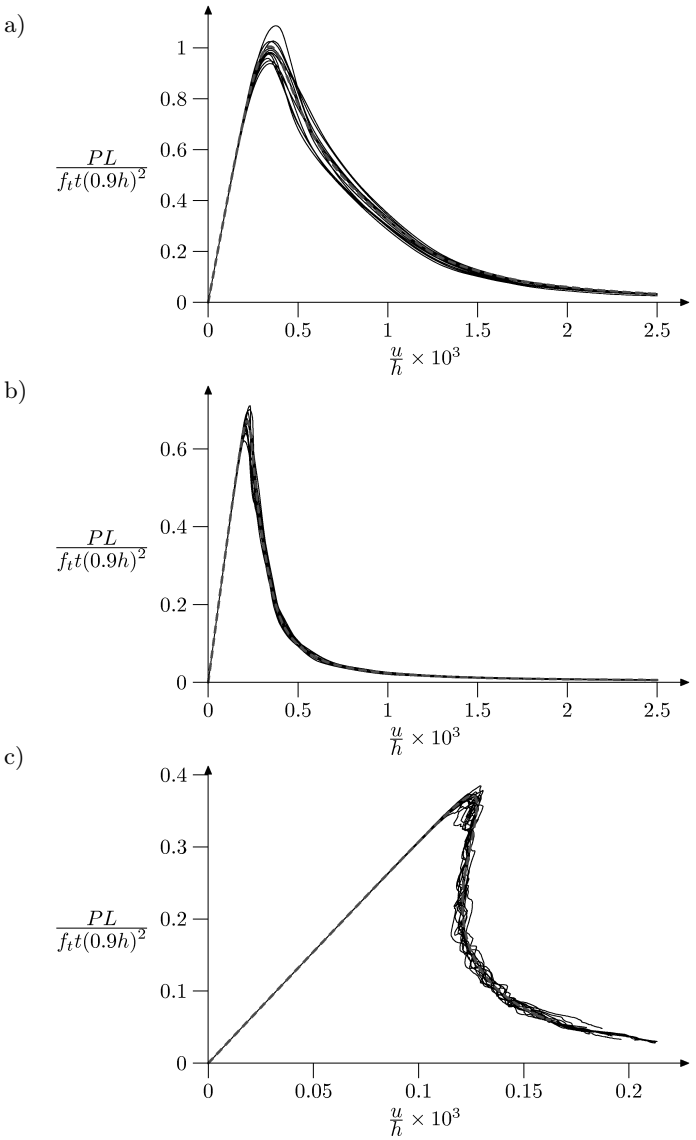

Fig. 12. Normalized force-displacement curves in the case of deterministic (dashed lines) and random calculation (solid lines) for 3 notched beams under three-point bending: a) small size beam ($h = 8$ cm), b) large size beam ($h = 32$ cm), c) very large size beam ($h = 192$ cm) ($\lambda_{x_1} = 1.0$ 1/m, $\lambda_{x_2} = 3.0$ 1/m, $s_{ft} = 0.424$ MPa).

and 192 cm (very large beam), respectively. Figure 13 demonstrates the calculated width of a localized zone. In turn, 5 arbitrary deformed FE-meshes for a small size beam are shown in Fig. 15.

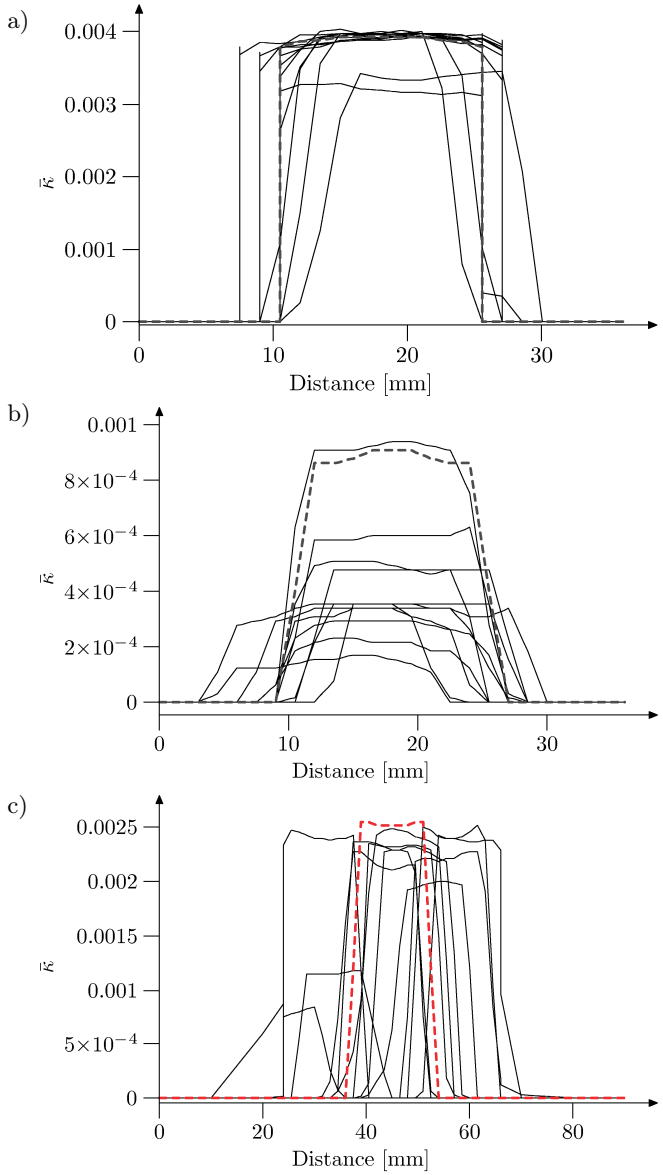

FIG. 13. Distribution of non-local softening parameter above the notch in the case of deterministic (dashed lines) and random calculation (solid lines) for 3 notched beams under three-point bending: a) small size beam ($h = 8$ cm), b) large size beam ($h = 32$ cm), c) very large size beam ($h = 192$ cm) ($\lambda_{x_1} = 1.0$ 1/m, $\lambda_{x_2} = 3.0$ 1/m, $s_{ft} = 0.424$ MPa).

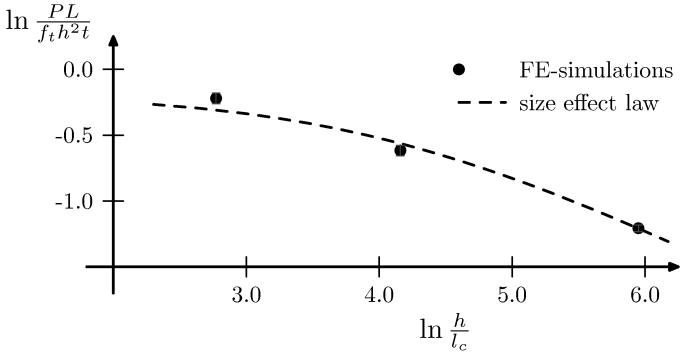

Fig. 14. Relationship between calculated normalized concrete strength $\ln\sigma = \ln[PL/(f_t h^2 t)]$ and ratio $\ln(h/l_c)$ compared to the size effect law by Bažant (Bažant and Planas [4]) for constant values of tensile strength.

The normalized maximum vertical force decreases with decreasing beam height h (Fig. 12). For $h = 8$ cm, it changes between 2.92–3.38 kN. The mean stochastic $P_{\max} = 3.08$ kN (with the standard deviation of 0.126 kN) is practically the same as the deterministic value $P_{\max} = 3.13$ kN (it is smaller by only 2%). If the beam height is $h = 32$ cm, the maximum vertical force varies between 7.73–8.85 and the mean stochastic force $P_{\max} = 8.30$ kN (with the standard deviation of 0.334 kN) is smaller by only 0.6% than the deterministic value ($P_{\max} = 8.35$ kN). For the beam height of $h = 192$ cm, the maximum vertical force varies between 26.05–28.72 kN and the mean stochastic $P_{\max} = 27.56$ kN is again smaller by only 0.6% than the deterministic value of $P_{\max} = 27.72$ kN (the standard deviation equals 0.692 kN). The load-displacement curves for a very large beam are not smooth in softening regime when tensile strength is distributed stochastically. The scatter of the maximum vertical force around its mean value is similar for all beam sizes (Fig. 14). The deformation field above the notch is strongly non-symmetric (Fig. 15). The mean width of the localized zone above the notch is slightly higher than the deterministic value, namely: w=16.56 mm ($h = 8$ cm), $w = 18.88$ mm ($h = 32$ cm) and $w = 19.67$ mm ($h = 192$ cm), Fig. 13.

Our results are similar to those given by Vořechovský [49]. However, in contrast to his results, the difference between stochastic and deterministic values and the scatter of stochastic values in our calculations were similar, independently of the beam size. It was caused by the assumption of a notch in our calculations contributing to the type-2 size effect (Bažant *et al.* [8]).

In contrast to simulations by Yang and Xu [50], which were performed with one notched beam only, the strong tortuousness of crack trajectories was not obtained in a small beam. Besides, the evolution of stochastic load-displacement curves was similar.

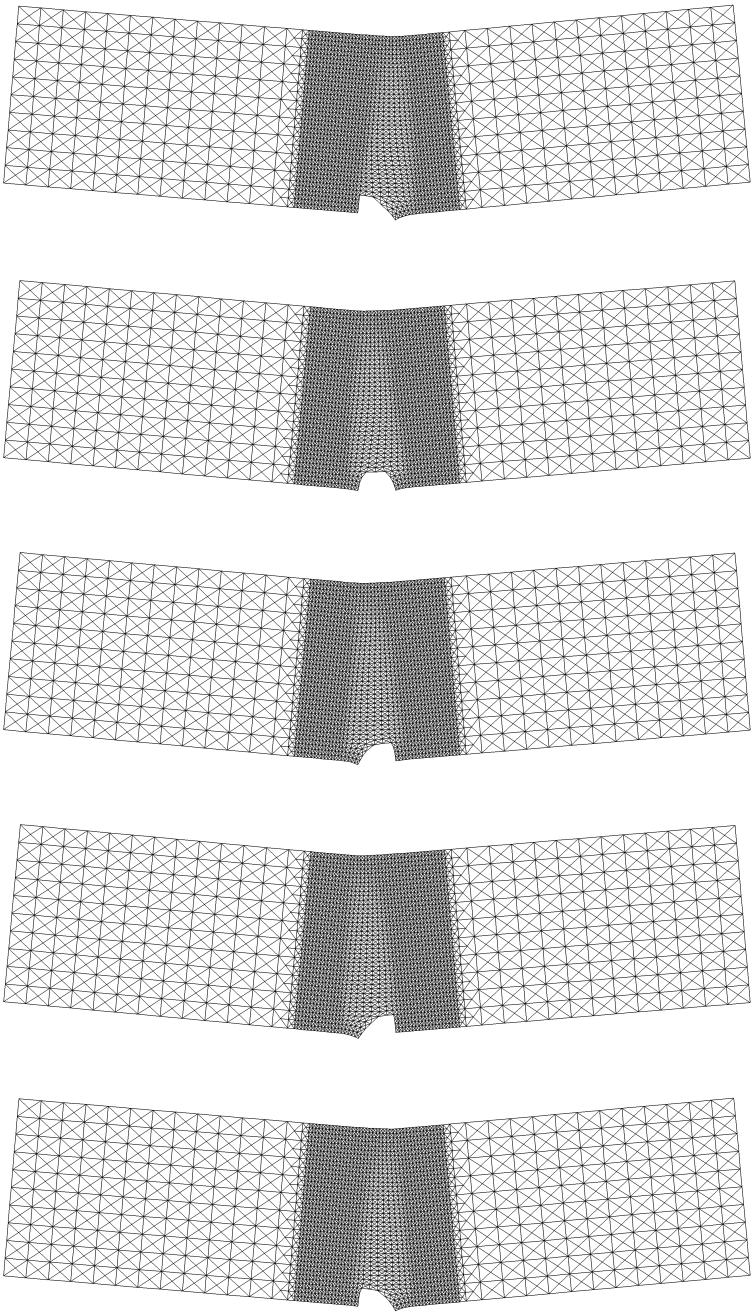

FIG. 15. Five arbitrary deformed FE meshes for a small size beam ($h = 8$ cm) $u/h = 0.25\%$) with random distribution of tensile strength ($\lambda_{x_1} = 1.0$ 1/m, $\lambda_{x_2} = 3.0$ 1/m. $s_{ft} = 0.424$ MPa.

Effect of samples' number

The calculations were carried out with a small size beam using a direct Monte Carlo method with 30 samples (Fig. 16) ($\lambda_{x_1} = 1.0$ 1/m, $\lambda_{x_2} = 3.0$ 1/m, $s_{f_t} = 0.424$ MPa). Almost similar results (mean $P_{\max} = 3.07$ kN with $s_P = 0.138$ kN) appeared as in the case of Latin hypercube sampling with 12 samples (mean $P_{\max} = 3.06$ kN).

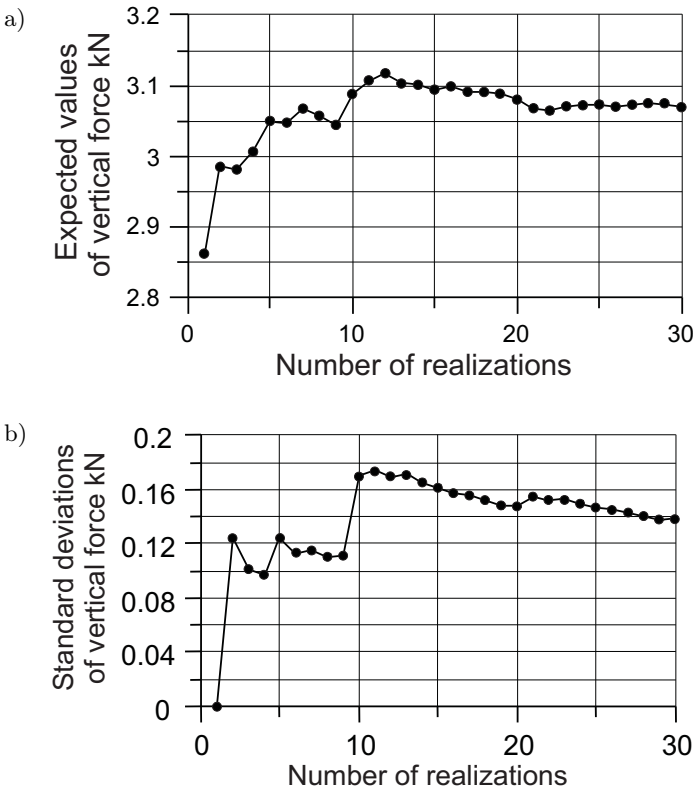

Fig. 16. Small size beam with random distribution of tensile strength ($h = 8$ cm) using a direct Monte Carlo method with 30 samples: maximum vertical force with expected values (a) and standard deviation (b) ($\lambda_{x_1} = 1.0$ 1/m, $\lambda_{x_2} = 3.0$ 1/m, $s_{ft} = 0.424$ MPa)

Effect of correlation range

In addition, the calculations were carried out with a small-size beam, assuming a very small correlation length of 10 mm (see Fig. 5) and $\lambda_{x_1} = 10.0$ 1/m, $\lambda_{x_2} = 10.0$ 1/m and $s_{f_t} = 0.424$ MPa in Eq. (3.1). The results (Figs. 17 and 18) show that the mean stochastic vertical force, $P_{\max} = 3.08$ kN, and mean width of the localized zone, $w = 16.56$ mm, are similar to the results with $\lambda_{x_1} = 1.0$ 1/m and $\lambda_{x_2} = 3.0$ 1/m. However, the scatter of forces is significantly smaller.

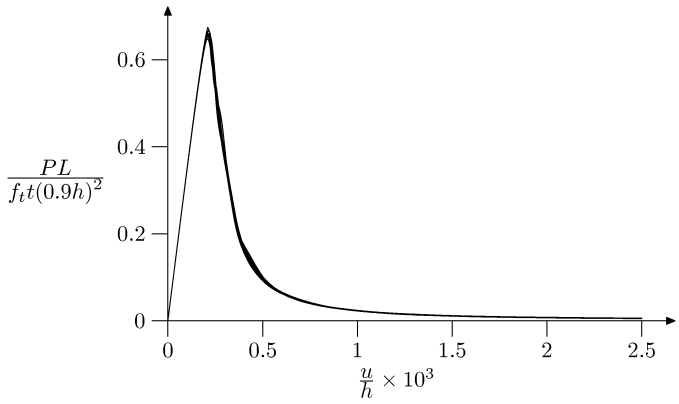

FIG. 17. Normalized force-displacement curves with and random distribution of tensile strength for notched small beam under three-point bending ($h = 8$ cm) for smaller correlation length ($\lambda_{x_1} = 10.0$ 1/m, $\lambda_{x_2} = 10.0$ 1/m, $s_{f_t} = 0.424$ MPa)

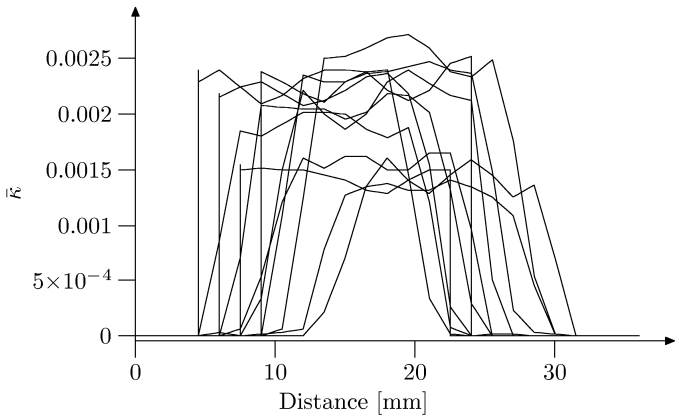

FIG. 18. Distribution of non-local softening parameter random distribution of tensile strength for notched small beam under three-point bending ($h = 8$ cm) for small correlation length ($\lambda_{x_1} = 10.0$ 1/m, $\lambda_{x_2} = 10.0$ 1/m, $s_{f_t} = 0.424$ MPa)

5. Conclusions

The following conclusions can be drawn from our non-linear FE-investigations of a deterministic and statistical size effect in notched concrete beams of a similar geometry:

The deterministic size effect (nominal strength decreases with increasing specimen size) is very pronounced. It is caused by occurrence of tensile localized zone above the notch with a certain width. The material ductility increases with decreasing specimen size. A pronounced snap-back behaviour occurs for

very large-size beams ($h/l_c \approx 400$). The width of the localized zone above the notch slightly increases with increasing beam size.

The solution of random non-linear problems on the basis of several samples is possible. The statistical size effect is significantly weaker than the deterministic one. The difference between deterministic material strength and mean statistical strength is practically negligible, independently of the beam size and correlation length.

The width of the localized zone above the notch in beams with a random distribution of tensile strength is slightly larger than that with constant values tensile strength due to a smaller rate of softening.

The scatter of the maximum force is similar in all beams. It decreases with decreasing correlation range.

Our research will be continued. In the next step, the size effects will be theoretically studied with unnotched concrete beams where a significantly stronger stochastic size effect is expected (Bažant and Planas [4]). The effect of the range of correlation and standard deviation of tensile strength will be studied again. In parallel, the experiments on size effects will be performed with beams of a different geometry by varying their height and length (Koide *et al.* [28]). A DIC technique will be applied to measure the width of the FPZ on the beam surface to calibrate the characteristic length (Skarzyński *et al.* [40]).

References

1. *Abaqus, Theory Manual*, Version 5.8, Hibbit, Karlsson & Sorensen Inc, 1998.
2. Z.P. Bažant, K.L. Lin, *Random creep and shrinkage in structures sampling*, J. Structural Engineering ASCE, **111**, 5, 1113–1134, 1985.
3. Z.P. Bažant, E.P. Chen, *Scaling of structural failure*, Applied Mechanics Reviews, **50**, 10, 593–627, 1997.
4. Z. Bažant, J. Planas, *Fracture and size effect in concrete and other quasi-brittle materials*, CRC Press LLC, 1998.
5. Z. Bažant, M. Jirasek, *Nonlocal integral formulations of plasticity and damage: survey of progress*, J. Engng. Mech., **128**, 11, 1119–1149, 2002.
6. Z. Bažant, *Probability distribution of energetic-statistical size effect in quasibrittle fracture*, Probabilistic Engineering Mechanics, **19**, 307–319, 2004.
7. Z.P. Bažant, A. Yavari, *Is the cause of size effect on structural strength fractal or energetic-statistical?* Engineering Fracture Mechanics **72**, 1–31, 2005.
8. Z. Bažant, M. Vořechovský, D. Novak, *Asymptotic prediction of energetic-statistical size effect from deterministic finite-element solutions*, J. Engineering Mechanics ASCE, **153**, 162, 2007.
9. E. Bielewicz, J. Górski, *Shell with random geometric imperfections. Simulation-based approach*, International Journal of Non-linear Mechanics, **37**, 4–5, 777–784, 2002.

10. J. BOBIŃSKI, J. TEJCHMAN, *Numerical simulations of localization of deformation in quasi-brittle materials within non-local softening plasticity*, Computers and Concrete, **4**, 433–455, 2004.

11. J. BOBIŃSKI, J. TEJCHMAN, *Modelling of size effects in concrete using elasto-plasticity with non-local softening*, Archives of Civil Engineering, **LII**, 1, 7–35, 2006.

12. J. BOBIŃSKI, J. TEJCHMAN, *Modelling of strain localization in quasi-brittle materials with coupled elasto-plastic-damage model*, J. Theoretical and Applied Mechanics, **44**, 4, 767–782, 2006.

13. R.B.J. BRINKGREVE, *Geomaterial models and numerical analysis of softening*, Phd Thesis, Delft University of Technology, 1994.

14. J. CARMELIET, H. HENS, *Probabilistic nonlocal damage model for continua with random field properties*, J. Engineering Mechanics ASCE, **120**, 2013–2027, 1994.

15. A. CARPINTERI, B. CHIAIA, G. FERRO, *Multifractal scaling law: an extensive application to nominal strength size effect of concrete structures*, [in:] Size effect of concrete structures M. MIHASHI, H. OKAMURA, Z.P. BAŽANT [Eds.], E&FN Spon, **173**, 185, 1994.

16. J. CHEN, H. YUAN, D. KALKHOF, *A nonlocal damage model for elastoplastic materials based on gradient plasticity theory*, Report No. 01-13, Paul Scherrer Institute, 1–130, 2001.

17. I. FERRARA, M. DI PRISCO, *Mode I fracture behaviour in concrete: nonlocal damage modeling*, ASCE Journal of Engineering Mechanics, **127**, 7, 678–692, 2001.

18. A. FLORIAN, *An efficient sampling scheme: Updated Latin hypercube sampling*, Probabilistic Engineering Mechanics, **2**, 123–130, 1992.

19. G.N. FRANTZISKONIS, *Stochastic modeling of hetereogeneous materials – a process for the analysis and evaluation of alternative formulations*, Mechanics of Materials, **27**, 165–175, 1998.

20. J. GÓRSKI, *Non-linear models of structures with random geometric and material imperfections simulation-based approach*, Gdansk University of Technology, **68**, 2006.

21. M.A. GUTIÉRREZ, R. DE BORST, *Energy dissipation, internal length scale and localization patterning – a probabilistic approach*, [in:] Computational Mechanics, S. IDELSOHN, E. ONATE, E. DVORKIN [Eds.], CIMNE, Barcelona, 1–9, 1998.

22. M.A. GUTIÉRREZ, *Size sensitivity for the reliability index in stochastic finite element analysis of damage*, International Journal of Fracture, **137**, 1–4, 109–120, 2006.

23. D.A. HORDIJK, *Local approach to fatigue of concrete*, PhD dissertation, Delft University of Technology, 1991.

24. T.J.R. HUGHES, J. WINGET, *Finite Rotation Effects in Numerical Integration of Rate Constitutive Equations Arising in Large Deformation Analysis*, Intern. Journal for Numerical Methods in Engineering, **15**, 1862–1867, 1980.

25. D.E. HUNTINGTON, C.S. LYRINTZIS, *Improvements to and limitations of Latin hypercube sampling*, Prob. Engng. Mech., **13**, No. 4, pp. 245–253, 1998.

26. J.E. HURTADO, A.H. BARBAT, *Monte Carlo techniques in computational stochastic mechanics*, Archives of Computational Method in Engineering, **5**, 1, 3–30, 1998.

27. W. KNABE, J. PRZEWŁÓCKI, G. RÓŻYŃSKI, *Spatial averages for linear elements for two-parameter random field*, Prob. Engng. Mech., **13**, 3, 147–167, 1998.

28. H. KOIDE, H. AKITA, M. TOMON, *Size effect on flexural resistance on different length of concrete beams*, Fracture Mechanics of concrete, H. MIHASHI, K. ROKUGP [Eds.], 2121–2130, 1998.

29. J. KOZICKI, J. TEJCHMAN, *Experimental investigations of strain localization in concrete using Digital Image Correlation (DIC) technique*, Archives of Hydro-Engineering and Environmental Mechanics, **54**, 1, 3–24, 2007.

30. C. LE BELLEGO, J.F. DUBE, G. PIJAUDIER-CABOT, B. GERARD, *Calibration of nonlocal damage model from size effect tests*, European Journal of Mechanics A/Solids, **22**, 33–46, 2003.

31. T. MAJEWSKI, J. BOBIŃSKI, J. TEJCHMAN, *FE-analysis of failure behaviour of reinforced concrete columns under eccentric compression*, Engineering Structures, **30**, 2, 300–317, 2008.

32. I. MARZEC, J. BOBIŃSKI, J. TEJCHMAN, *Simulations of crack spacing in reinforced concrete beams using elastic-plasticity and damage with non-local softening*, Computers and Concrete, **4**, 5, 377–403, 2007.

33. M.D. MCKAY, W.J. CONOVER, R.J. BECKMAN *A comparison of three methods for selecting values of input variables in the analysis of output from a computer code*, Technometrics **21**, 239–245, 1979.

34. J. VAN MIER, M. VAN VLIET, *Influence of microstructure of concrete on size/scale effects in tensile fracture*, Engineering Fracture Mechanics, **70**, 2281–2306, 2003.

35. J. PAMIN, R. DE BORST, *Simulation of crack spacing using a reinforced concrete model with an internal length parameter*, Arch. App. Mech., **68**, 9, 613–625, 1998.

36. J. PAMIN, *Gradient-enhanced continuum models: formulation, discretization and applications*, Habilitation Monography, Cracow University of Technology, Cracow 2004.

37. G. PIJAUDIER-CABOT, Z.P. BAŽANT, *Nonlocal damage theory*, ASCE J. Eng. Mech., **113**, 1512–1533, 1987.

38. G. PIJAUDIER-CABOT, K. HAIDAR, J.F. DUBE, *Non-local damage model with evolving internal length*, Int. J. Num. and Anal. Meths. in Geomech., **28**, 633–652, 2004.

39. A. SIMONE, G.N. WELLS, L.J. SLUYS, *From continuous to discontinuous failure in a gradient-enhanced continuum damage model*, Computer Methods in Applied Mechanics and Engineering, **192**, 4581–4607, 2003.

40. L. SKARZYŃSKI, E. SYROKA, J. TEJCHMAN, *Measurements and calculations of the width of the fracture process zones on the surface of notched concrete beams*, Strains, doi: 10.1111/j.1475-1305.2008.00605.x, 2009.

41. J. TEJCHMAN, J. GÓRSKI, *Computations of size effects in granular bodies within micropolar hypoplasticity during plane strain compression*, Int. J. for Solids and Structures, **45**, 6, 1546–1569 2007.

42. J. TEJCHMAN, J. GÓRSKI, *Deterministic and statistical size effect during shearing of granular layer within a micro-polar hypoplasticity*, Intern. Journal for Numerical and Analytical Methods in Geomechanics, **32**, 1, 81–107, 2008.

43. J. WALRAVEN, N. LEHWALTER, *Size effects in short beams loaded in shear*, ACI Structural Journal, **91**, 5, 585–593, 1994.

44. H. WALUKIEWICZ, E. BIELEWICZ, J. GÓRSKI, *Simulation of nonhomogeneous random fields for structural applications*, Computers and Structures, **64**, 1–4, 491–498, 1997.

45. W. WEIBULL, *A statistical theory of the strength of materials*, Journal of Applied Mechanics, **18**, 9, 293–297, 1951.

46. F.H. WITTMANN, H. MIHASHI, N. NOMURA, *Size effect on fracture energy using three-point bend tests*, Materials and Structures, **25**, 327–334, 1992.

47. E.-H. VANMARCKE, *Random Fields: Analysis and Synthesis*, Cambridge: MIT Press, 1983.

48. M.R.A. VAN VLIET, *Size effect in tensile fracture of concrete and rock*, PhD thesis, University of Delft, 2000.

49. M. VOŘECHOVSKÝ, *Interplay of size effects in concrete specimens under tension studied via computational stochastic fracture mechanics*, Int. J. Solids and Structures, **44**, 2715–2731, 2007.

50. Z. YANG, X.F. XU, *A heterogeneous cohesive model for quasi-brittle materials considering spatially varying random fracture properties*, Computer Methods in Applied Mechanics and Engineering, **197**, 45–48, 4027–4039, 2008.

51. Q. YU, *Size effect and design safety in concrete structures under shear*, PhD Thesis, Northwestern University, 2007.

Received November 17, 2008; revised version May 5, 2009.